FULL LENGTH ARTICLE

The Anatomical Record
Advances in Integrative Anatomy and Evolutionary Biology

WILEY

Development and growth of the pelvic fin in the extant coelacanth *Latimeria chalumnae*

Rohan Mansuit[1,2] (ID) | Gaël Clément[1] | Anthony Herrel[2] (ID) | Hugo Dutel[3,4] (ID) |
Paul Tafforeau[5] (ID) | Mathieu D. Santin[6] (ID) | Marc Herbin[2]

[1]Département Origines and Evolution, UMR 7207 Centre de Recherche en Paléontologie, Paris, MNHN - Sorbonne Université - CNRS, Paris, France

[2]Département Adaptations du Vivant, UMR 7179 MECADEV, MNHN - CNRS, Paris, France

[3]School of Earth Sciences, University of Bristol, Bristol, UK

[4]School of Engineering and Computer Science, University of Hull, Hull, UK

[5]European Synchrotron Radiation Facility, Grenoble Cedex, France

[6]Inserm U 1127, CNRS UMR 7225, Centre for NeuroImaging Research, ICM (Brain & Spine Institute), Sorbonne University, Paris, France

Correspondence
Rohan Mansuit, Département Adaptations du Vivant, UMR 7179 MECADEV, MNHN - CNRS, 55 rue Buffon, 75005 Paris, France.
Email: rohan.mansuit@mnhn.fr

Funding information
Agence Nationale de la Recherche in the LabEx ANR-10-LABX-0003-BCDiv, Grant/Award Number: ANR-11-IDEX-0004-02

Abstract

The ontogeny of the paired appendages has been extensively studied in lungfishes and tetrapods, but remains poorly known in coelacanths. Recent work has shed light on the anatomy and development of the pectoral fin in *Latimeria chalumnae*. Yet, information on the development of the pelvic fin and girdle is still lacking. Here, we described the development of the pelvic fin and girdle in *Latimeria chalumnae* based on 3D reconstructions generated from conventional and X-ray synchrotron microtomography, as well as MRI acquisitions. As in other jawed vertebrates, the development of the pelvic fin occurs later than that of the pectoral fin in *Latimeria*. Many elements of the endoskeleton are not yet formed at the earliest stage sampled. The four mesomeres are already formed in the fetus, but only the most proximal radial elements (preaxial radial 0–1) are formed and individualized at this stage. We suggest that all the preaxial radial elements in the pelvic and pectoral fin of *Latimeria* are formed through the fragmentation of the mesomeres. We document the progressive ossification of the pelvic girdle, and the presence of a trabecular system in the adult. This trabecular system likely reinforces the cartilaginous girdle to resist the muscle forces exerted during locomotion. Finally, the presence of a preaxial element in contact with the pelvic girdle from the earliest stage of development onward questions the mono-basal condition of the pelvic fin in *Latimeria*. However, the particular shape of the mesomeres may explain the presence of this element in contact with the girdle.

KEYWORDS

Actinistia, appendages, endoskeleton, ontogeny, sarcopterygians

1 | INTRODUCTION

Among sarcopterygians, the living coelacanths *Latimeria chalumnae* (Smith, 1939) and *L. menadoensis* (Pouyaud et al., 1999) are the only living representatives of the Actinistia, a clade closely related to lungfishes and tetrapods (Amemiya et al., 2013; Clack, 2012; Forey, 1998;

Friedman, Coates, & Anderson, 2007). Although the anatomy of *Latimeria chalumnae* is well known (Millot & Anthony, 1958, 1965; Millot, Anthony, & Robineau, 1978), its development remains largely unknown. Indeed, only a few embryos and one juvenile are present in collections worldwide (Nulens, Scott, & Herbin, 2011). Due to the improvement of noninvasive imaging techniques such as conventional and synchrotron micro-tomography, as well as magnetic resonance imaging, it is now possible to study the development of small and complex internal structures of the coelacanth like the lung (Cupello et al., 2015), the neurocranium (Dutel et al., 2019) and the pectoral fin (Mansuit et al., 2019).

The endoskeleton elements of the paired fins or limbs are organized along a single metapterygial axis in sarcopterygians (Millot & Anthony, 1958; Shubin & Alberch, 1986). However, whereas the development of paired appendages in lungfishes and tetrapods is relatively well known (Boisvert, Joss, & Ahlberg, 2013; Jude, Johanson, Kearsley, & Friedman, 2014; Shubin & Alberch, 1986), it remains poorly studied in coelacanths (but see (Mansuit et al., 2019). Yet, the development of the pelvic appendages of vertebrates occurs later than the pectoral appendages (Cubbage & Mabee, 1996; Mabee & Noordsy, 2004; Mabee & Trendler, 1996). Therefore, documenting the development of the pelvic fin of *Latimeria* is important to fully understand the development of the paired fins in this species. Following our recent work on pectoral fin development (Mansuit et al., 2019), we here describe the anatomy and development of the pelvic appendage of *Latimeria* based on an ontogenetic series of five different stages.

2 | MATERIALS AND METHODS

2.1 | Specimens

The developmental series includes five stages including specimens from several Museum collections (Figure 1). The first stage is a fetus of 5 cm total length (TL) (international number: CCC 202.1) found inside the female specimen CCC 202 captured off the coast of Tanzania in 2005 and conserved in the collection of the South African Institute for Aquatic Biodiversity (SAIAB) in Grahamstown (collection number: SAIAB 76199). The stage two is a pup with yolk sac of 32.3 cm TL (CCC 29.5) found inside the female specimen CCC 29 captured in the Comores in 1969 and conserved in the collection of the Muséum national d'Histoire naturelle (MNHN), Paris (collection number: MNHN AC 2012-22). The stage three is a late pup without a yolk sac of 34.8 cm TL (CCC 162.21) found inside the female CCC 162 captured off the coast of Mozambique in 1991 and conserved in the collections of the Zoologische Staatssammlung of Munich (collection number: ZSM 28409). The stage four is a juvenile of 42.5 cm TL (CCC 94) captured off the coast of Grande Comore Island in 1974 and conserved in the collections of the MNHN, Paris (collection number: MNHN AC 2012-27). Imaging reconstructions and observations on adult stage (Stage 5) were mainly based on a male specimen of 132 cm TL (CCC 27) captured off the coast of Grande Comore Island in 1961 and conserved in the collections of the MNHN, Paris (collection number: MNHN AC 2012-21) (Nulens et al., 2011). Direct anatomical observations were also made from on a dissected and prepared pelvic fin skeleton of adult specimen CCC 7 (collection number: MNHN
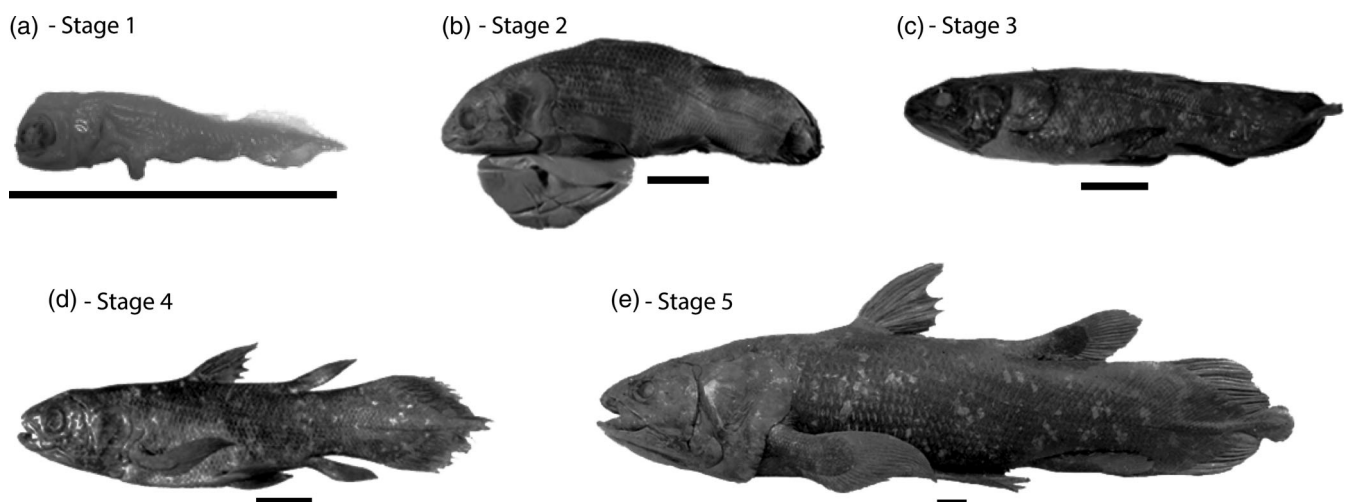

FIGURE 1 *Latimeria chalumnae*—Ontogenetic series in left lateral view. (a) Early embryo (CCC 202.1), (b) Embryo with yolk sac (CCC 29.5), (c) Late embryo without yolk sac (CCC 162.21), (d) Juvenile (CCC 94), (e) Adult (CCC 27). Scale bar = 5 cm

AC 2012-5). All specimens of the MNHN, Paris are conserved in a 6–7% formaldehyde solution, while the others are preserved in an aqueous ethanol solution (70%).

2.2 | Imaging

Figure 2 illustrates sections through the girdle and fins of the different specimens illustrating the quality of the raw data used in this article.

2.2.1 | Stage 1: Fetus (CCC 202.1)

The specimen was scanned using long propagation phase-contrast synchrotron X-ray microtomography at
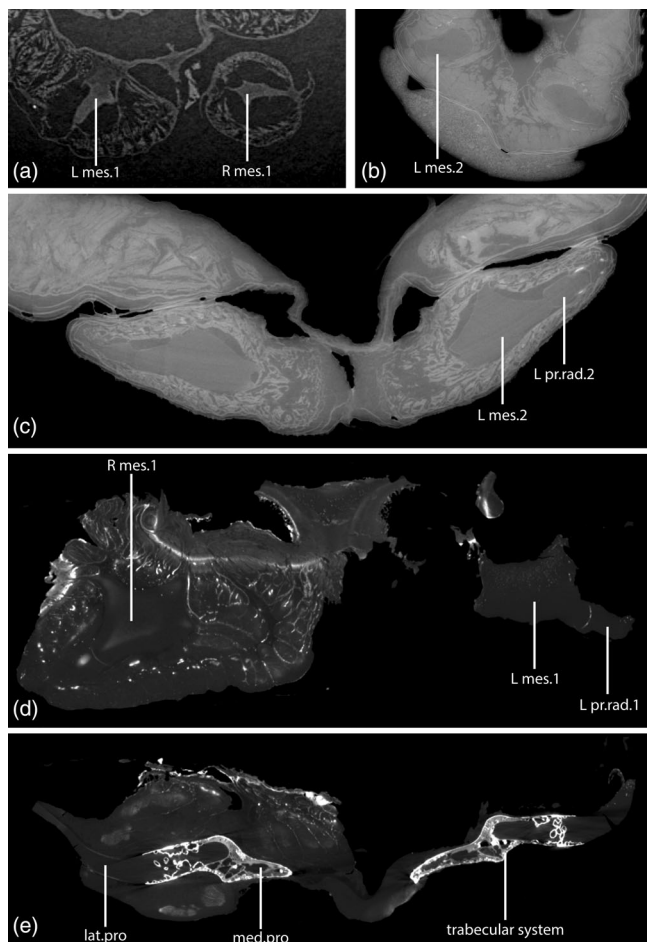

FIGURE 2 Transverse section of the pelvic fin and girdle in the fetus (a), pup 1 (b), pup 2 (c), and adult (d, e) showing the quality of the scans and the contrast for the different stages, at different section along the fin. Transverse section for the fetus, pup 1, and 2 are zoomed on the pelvic fin (a, b, c). Concerning the adult stage, the pelvic fins were isolated and the left fin was dissected (d, e). lat.pro., lateral process; med.pro., medial process; mes., mesomere; pr.rad., preaxial radial

the ID19 beamline of the European Synchrotron Radiation Facility (ESRF), Grenoble (France). It was imaged in a glass cylinder filled with ethanol, at a voxel size of 6.5 μm, with a high-quality pink beam using the ID19 W150 wiggler and a gap of 50 mm filtered by 2 mm of aluminum, 0.25 mm of copper, and 0.2 mm of gold. The scintillator was a 250-μm-thick LuAG:Ce (lutetium–aluminum–garnet) crystal. The resulting detected spectrum was then centered on 77 keV, with a bandwidth of 17 keV full width at half maximum (FWHM). The detector was a FreLoN 2K charge-coupled device (CCD) camera mounted on a lens system. To obtain a sufficient propagation phase-contrast effect, a distance of 3 m between the sample and the detector was used. Synchrotron data were reconstructed using a filtered back-projection algorithm coupled with a single distance phase-retrieval process (Paganin, Mayo, Gureyev, Miller, & Wilkins, 2002; Sanchez, Ahlberg, Trinajstic, Mirone, & Tafforeau, 2012). All the sub-scans were reconstructed separately, converted into 16-bit TIFF stacks and then concatenated to generate a single complete volume. The ring artifacts were corrected on the reconstructed slices using a specific tool developed at the ESRF (Lyckegaard, Johnson, & Tafforeau, 2011). The final volume used for the present study (13 μm voxel size) was obtained after isotropic 2-times binning with the software ImageJ.

2.2.2 | Stage 2: Pup 1 (with yolk sac) (CCC 29.5)

The specimen was scanned on the ID19 beamline on the ESRF in an empty plastic tube, at a voxel size of 23.34 μm, using a propagation distance of 13 m to maximize the phase-contrast effect. The beam produced by the W150 wiggler at a gap of 59 mm was filtered by 2.8 mm of aluminum and 1.4 mm of copper, resulting in an average detected energy of 77.4 keV. The scintillator was a 2000-μm-thick LuAG:Ce (lutetium–aluminum–garnet doped with cerium) crystal. The detector was a PCO edge 4.2 sCMOS. Tomographic slices were reconstructed using the same protocol as the one described above. The final volume (46.68 μm voxel size) was obtained after isotropic 2-times binning with the software ImageJ.

2.2.3 | Stage 3: Pup 2 (with yolk sac resorbed) (CCC 162.21)

The specimen was scanned in a similar manner to Stage 2, at a voxel size of 23.34 μm. The scintillator, detector, and distance between the sample and the detector were the same as for the stage 2 embryo. The final volume

(46.68 μm voxel size) was obtained after isotropic 2-times binning in ImageJ.

2.2.4 | Stage 4: Juvenile (CCC 94)

The specimen was scanned twice, once at the ESRF on the beamline ID19 and once using magnetic resonance imaging (MRI). At the ESRF, the specimen was scanned in a plastic tube filled with water, at a voxel size of 28.43 μm, using a propagation distance of 13 m to maximize the phase-contrast effect. The beam produced by the W150 wiggler at a gap of 30 mm was filtered by 2 mm of aluminum and 15 mm of copper, resulting in an average detected energy of 170 keV with a bandwidth of 85 keV FWHM. The detector camera was a FreLoN 2K charge-coupled device mounted on a lens system coupled to a 750-mm-thick LuAG:Ce scintillator. Tomographic slices were reconstructed using the same protocol as the ones described above. The final volume (56.86 μm voxel size) was obtained after isotropic 2-times binning with the software ImageJ.

As the contrast was not sufficient due to the partial demineralization of the bones linked to the long preservation in formalin solution, the specimen was re-scanned using MRI at a lower resolution. The MRI was performed at 3T with a Siemens Tim TRIO (Siemens, Germany) system. Images were acquired with a 3D Flash sequence using an isotropic resolution of 300 μm. Parameters were matrix size = 640 × 300 × 256, TR/TE (msec) = 18/4.73, flip angle = 10°, spectral width = 100 kHz, number of averages = 20, total acquisition time was 7 hr, and 41 min.

2.2.5 | Stage 5: Adult (CCC 27)

The specimen CCC 27 was scanned at the AST-RX facility of the MNHN (Paris, France) using the stacking of multiple scans with the following scanning parameters: voltage 110 kV, current 950 μA, filter 0.2 mm Cu, voxel size 105 μm, and 3,258 views.

2.3 | Segmentation and 3D-reconstruction method

For all the specimens, segmentation and three-dimensional rendering were done using the software MIMICS Innovation Suite 20.0 (Materialise) (Stages 1–4) and MIMICS Innovation Suite 21.0 (Materialise) (Stage 5). The different objects were exported in STL format and transformed into a 3D PDF with the software 3-matic 11.0 (Materialise) (Stages 1–4) and 3-matic 13.0 (Materialise) (Stage 5).

3 | RESULTS

The pelvic appendages are located on the ventral side of the animal, in the middle of the body on both sides of the cloaca (Millot et al., 1978).

3.1 | The pelvic girdle

In the adult stage, the pelvic girdle is a massive element and supports several processes: the anterior process (ant.p) ("segment antérieur" according to Millot and Anthony), the lateral process (lat.pro.) ("apophyse latérale externe" according to Millot and Anthony), the medial process (med.pro) ("apophyse latérale interne" according to Millot and Anthony), and the posterosuperior process (ps.pro) ("apophyse postéro-supérieure" according to Millot and Anthony) (Figures 2e and 3). The anterior process is a long cartilaginous and rod-like structure that gently flares anteriorly to form a flattened blade. The lateral process is large and flat, concave on its dorsal side, with an anterior peak, whereas the medial process is a short and triangular expansion. The posterosuperior process is robust and short, with a flattened apex. The posterior part of the girdle presents a convex articular head, called the acetabulum, which articulates with the first axial element of the fin. The two girdles are not fused in *Latimeria* (Figure 4c) but joined by ligaments between the two medial processes and between the distal edges of the two anterior processes. The microtomographic data allow, for the first time, the visualization of a partially denser region at the surface of the pelvic girdle that could correspond to an endochondral ossification of the girdle (Figures 2e–4). In the adult, this region covers the anterior process, the medial process, and extends posteriorly until the base of the posterosuperior process and of the lateral process with a convex expansion. This denser area is internally associated with a trabecular system (Figures 2e–4b) that is well developed in the posterior part and the medial process of the girdle. The anterior process and the base of the lateral process present a trabecular system that appears to be less developed. This ossification is also visible on the isolated pelvic girdle of the specimen CCC 7.

In the fetus, the pelvic girdle is relatively smaller and shows a very different shape from what is observed in the next stages (Figure 5a). The different processes have morphologies different from those observed in the adult stage. The anterior process of the girdle is only represented by a small pointed extension. The medial process is large with a square shape and the lateral process forms only a short crest. The posterosuperior process is a reduced convex process. From pup 1 onward, the girdle becomes more complete and all its processes are fully formed (Figure 5b–e).
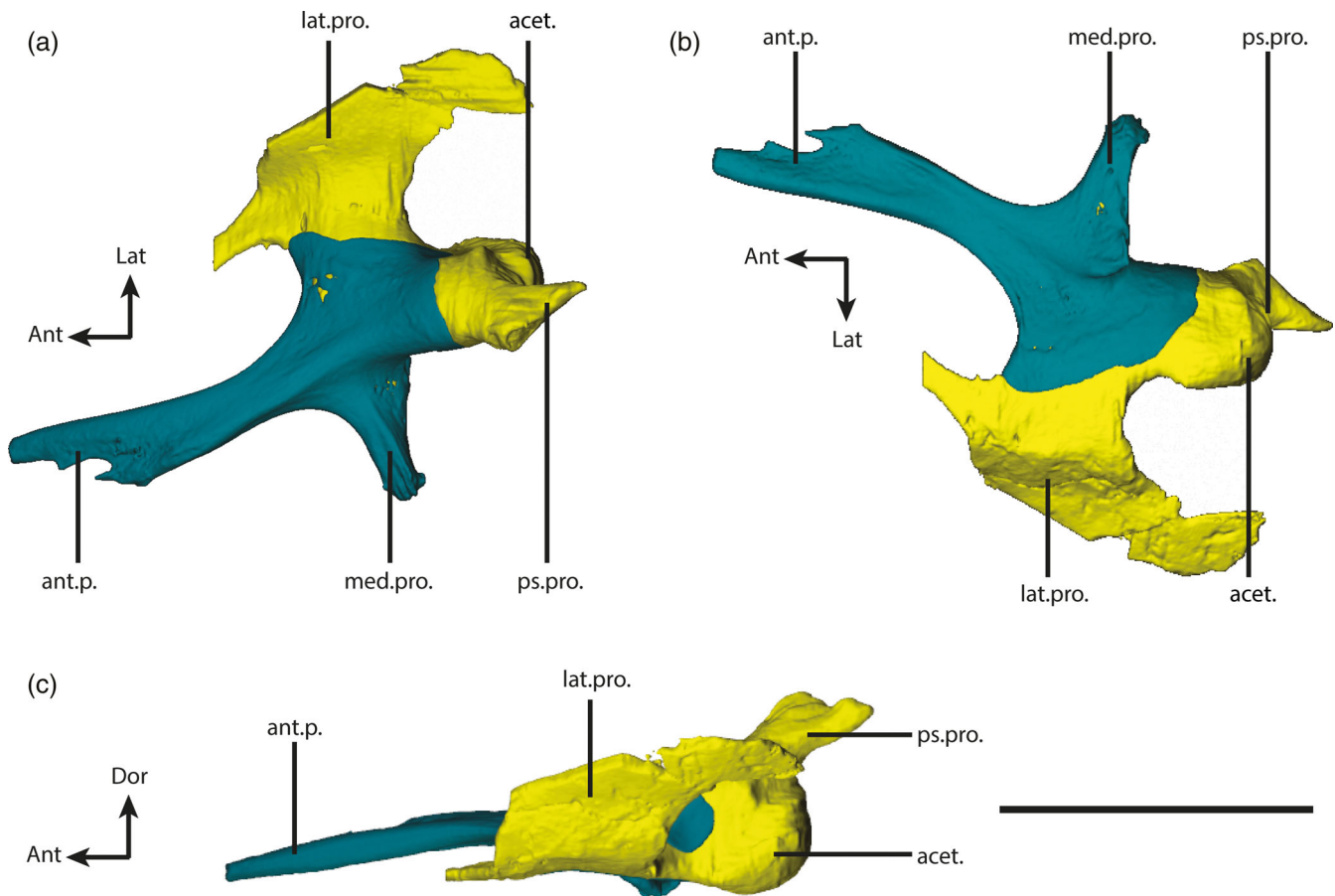
FIGURE 3 *Latimeria chalumnae*—Adult stage. Right pelvic girdle in dorsal view (a), ventral view (b), and lateral view (c). act., acetabulum; ant.p., anterior process; lat.p., lateral process; med.pro., medial process; pos.p., posterior part; ps.pro., posterosuperior process. Blue = dense part of the girdle; yellow = endoskeletal pelvic girdle. Scale bar = 50 mm

In pup 1, the anterior process of the right girdle does not form a blade, but a bifid process. The dense superficial surface only partially covers the anterior process of the girdle (Figure 5b). From pup 2 onward, the anterior process of the girdle forms a blade. The dense superficial surface covers almost the entire anterior process of the girdle and the most anterior part of the girdle (Figure 5c). In the juvenile, the ossification expands to the posterior part of the girdle and partially covers the medial process (Figure 5d). No trabecular system can be observed, in contrast to the adult stage.

3.2 | The pelvic fin

The pelvic fin (Figure 6) is composed of several elements: mesomeres on the metapterygial axis, preaxial elements (preaxial radials + preaxial accessory elements), and postaxial elements (postaxial radials + distal radial). According to Millot and Anthony (1958), the metapterygial axis of the fin consists of five axial elements (named "*articles*"), numbered from proximal to distal, while Forey (1998) identified four mesomeres and one distal radial element. There

are five preaxial radial elements (Forey, 1998; Millot & Anthony, 1958), a variable number of preaxial accessory elements, and postaxial radials (Millot & Anthony, 1958). The fin rays insert on the preaxial and postaxial elements of the fin (see descriptions below). As described by Millot and Anthony (1958), the so-called "fifth article" of the metapterygial axis has a different shape compared to the previous elements of the metapterygial axis, and the fin rays insert on it. Following Forey (1998), we, therefore, consider this element as a distal radial belonging to the postaxial elements (Figure 6). In the adult stage, the organization of the endoskeleton of the pelvic fin is similar to that observed for the pectoral fin (Mansuit et al., 2019; Millot & Anthony, 1958) (Figure 7). However, unlike in the pelvic girdle, there is no trabecular system in any element of the pelvic fin (as for the pectoral fin) (Figure 2).

3.2.1 | The metapterygial axis

As for the pectoral fin of *L. chalumnae* (Mansuit et al., 2019), we use the term mesomere for subcylindrical
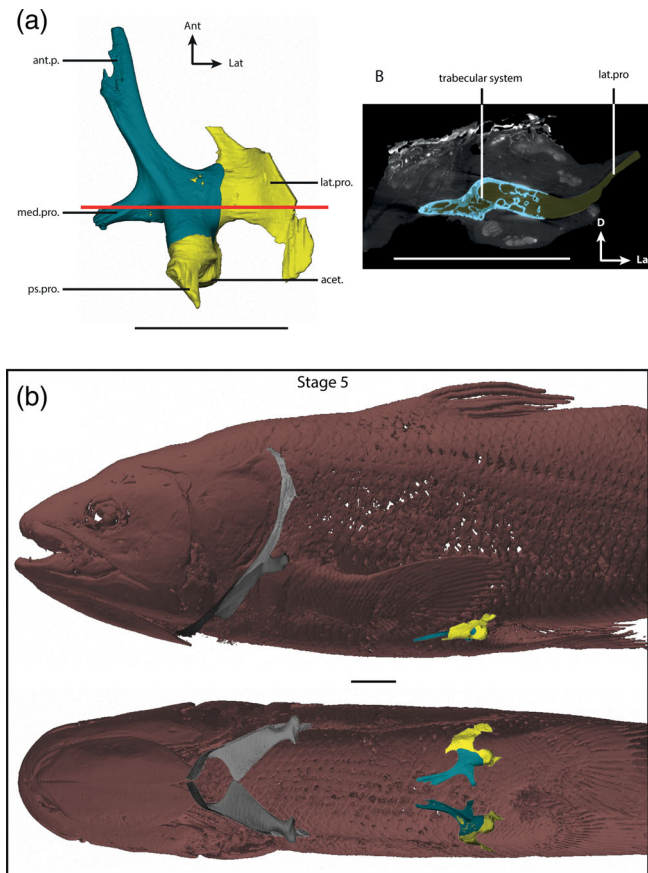
FIGURE 4 *Latimeria chalumnae*—Adult stage. Right pelvic girdle in dorsal view (a) and transverse section (b). Location of the pectoral and pelvic girdle inside the body in the left and ventral view (c). The red line in A shows the location of the transverse section. The trabecular system and the dense radio-opaque part of the girdle are clearly visible. The color code of the transverse section and the 3D model is identical. act., acetabulum; ant.p., anterior process; lat.p., lateral process; med.pro., medial process; pos.p., posterior part; ps.pro., posterosuperior process. Blue = dense part of the pelvic girdle; yellow = endoskeletal pelvic girdle; grey = pectoral girdle. Scale bar = 50 mm

radial segments of the principal axis in sarcopterygian fins (Jarvik, 1980).

As described by Millot and Anthony (1958) for the adult stage, the four mesomeres have a similar length, and the three first mesomeres have a similar shape (Figure 6a). There is a progressive dorsoventral flattening of the mesomeres from proximal to distal (Figure 6b). From proximal to distal, the ridges on the dorsal side of the mesomeres are also progressively less developed and have an increasingly medial position from the first to the third mesomere.

3.2.2 | The first mesomere (mes.1)

As described by Millot and Anthony (1958) in the adult stage the first mesomere is wider than long and slightly

arc-shaped. It articulates with the acetabulum of the pelvic girdle by its concave proximal edge and with the next mesomere by its convex distal edge (Figure 6). The angle between the distal edge and the medial edge forms a large process. The dorsal side presents a strong but irregular oblique crest, directed from proximo-lateral to disto-medial. The ventral facet of the mesomere is flatter with only a small swelling on the medial part of its surface.

In the fetus, the shape of the first mesomere is similar to that seen in the adult specimen: concave on the proximal edge and convex on the distal edge, with a ridge on its dorsal face (Figure 7a). There is a bilateral asymmetry to the morphology of the mesomere, since the ridge is oblique on the right fin whereas it is longitudinal on the left fin (Figure 10a). This first mesomere is squarer in the fetus than in the adult stage. There is no process on the medial side of the mesomere. The ventral side of the mesomere does not have a swelling on the medial part of the surface, but a longitudinal ridge close to the medial edge. From pup 1 onward, the first mesomere has already its adult shape, arc-shaped and slightly wider than long (Figure 7b–e). The dorsal ridge is well developed, with an irregular surface. In pup 1, the ventral face of the first mesomere has an important swelling on the medial part of its surface. From pup 2 onward, the swelling is less important and the ventral side of the mesomere is flatter. The oblique crest on the ventral face of this mesomere described by Millot and Anthony (1958) is not present from pup 1 onward, neither is it on the isolated pelvic fin.

3.2.3 | The second mesomere (mes.2)

In the adult stage, the second mesomere has a morphology similar to that of the first mesomere, but more flattened and slightly shorter (Figure 6). The medial process is smaller and the dorsal ridge less developed. The latter is less oblique and more latero-medially oriented than on the mesomere 1.

In the fetus, the second mesomere is trapezoid in shape. There is no process on its medial edge, and the ridge is poorly developed (Figure 7a). Moreover, this ridge is longitudinal on the left fin whereas it is more oblique on the right fin (Figure 10a). From pup 1 onward, the second mesomere has its adult shape (Figure 7b–e). As for the first mesomere, the swelling surface on the ventral face of the second mesomere is well marked in pup 1, yet becomes flatter from pup 2 onward.

3.2.4 | The third mesomere (mes.3)

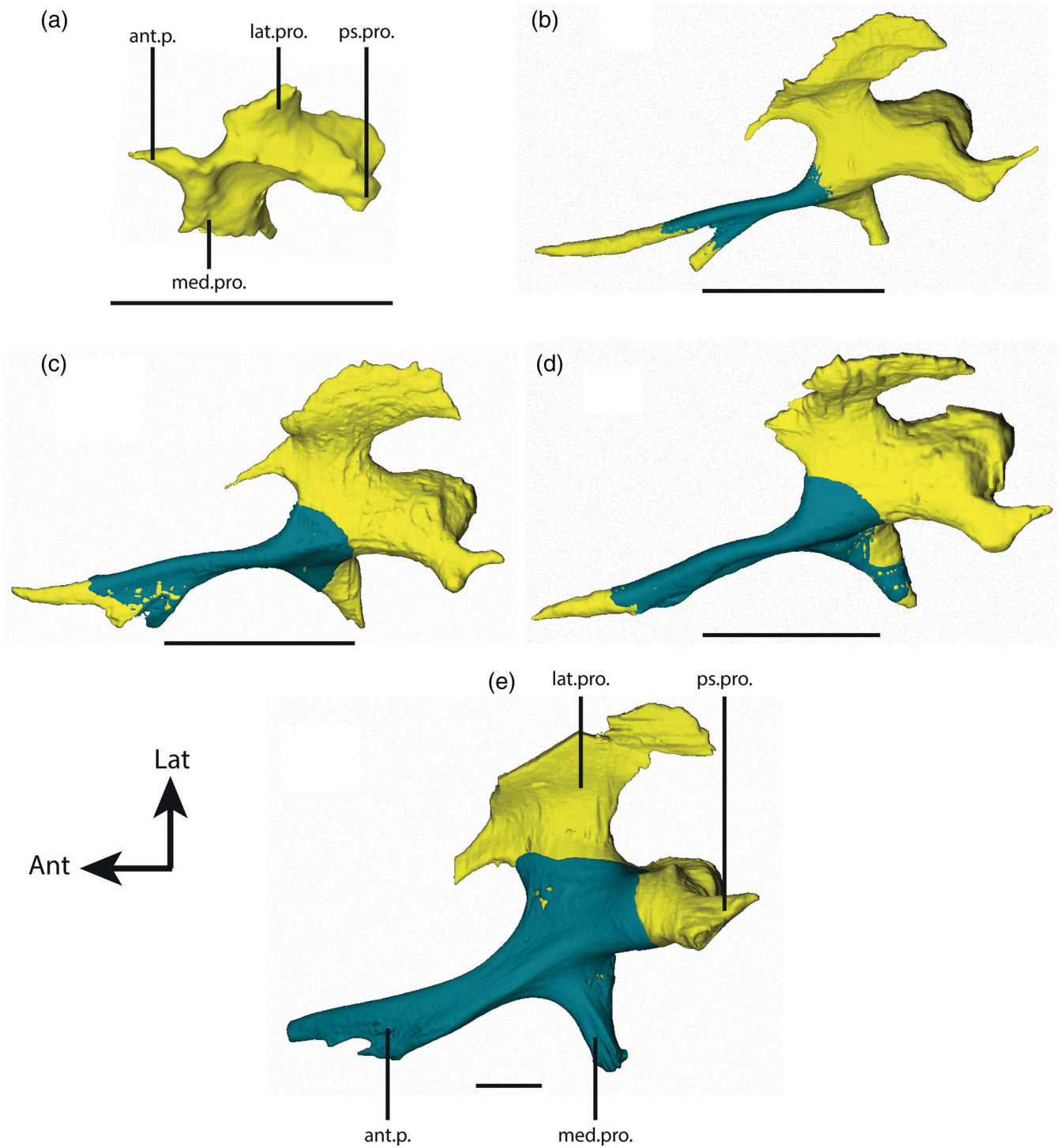In the adult stage, the length of this element is smaller than those of previous mesomeres, but the width is more

FIGURE 5 *Latimeria chalumnae*. Right pelvic girdle in dorsal view at five different developmental stages. a: Stage 1, b: Stage 2, c: Stage 3, d: Stage 4, and e: Stage 5. ant.p., anterior process; lat.p., lateral process; med.pro., medial process; pos.p., posterior part; ps.pro., posterosuperior process. Blue = dense part of the girdle; yellow = endoskeletal pelvic girdle. a: Scale 2 mm; b–e: Scale bar = 10 mm

or less the same (Figure 6). The general morphology is boomerang-liked. Like for the previous mesomeres the dorsal ridge is well developed, but less pronounced. However, the medial process is barely visible.

In the fetus, the third mesomere is square in shape, with a proximo-lateral extension (Figure 7a). This extension could correspond to the second preaxial radial in a fragmentation process of this early mesomere. The dorsal ridge is longitudinal and in medial position. From pup 1 onward, the third mesomere has its boomerang shape and its well-developed ridge, as in the adult (Figure 7b–e). As for the previous mesomeres, the ventral
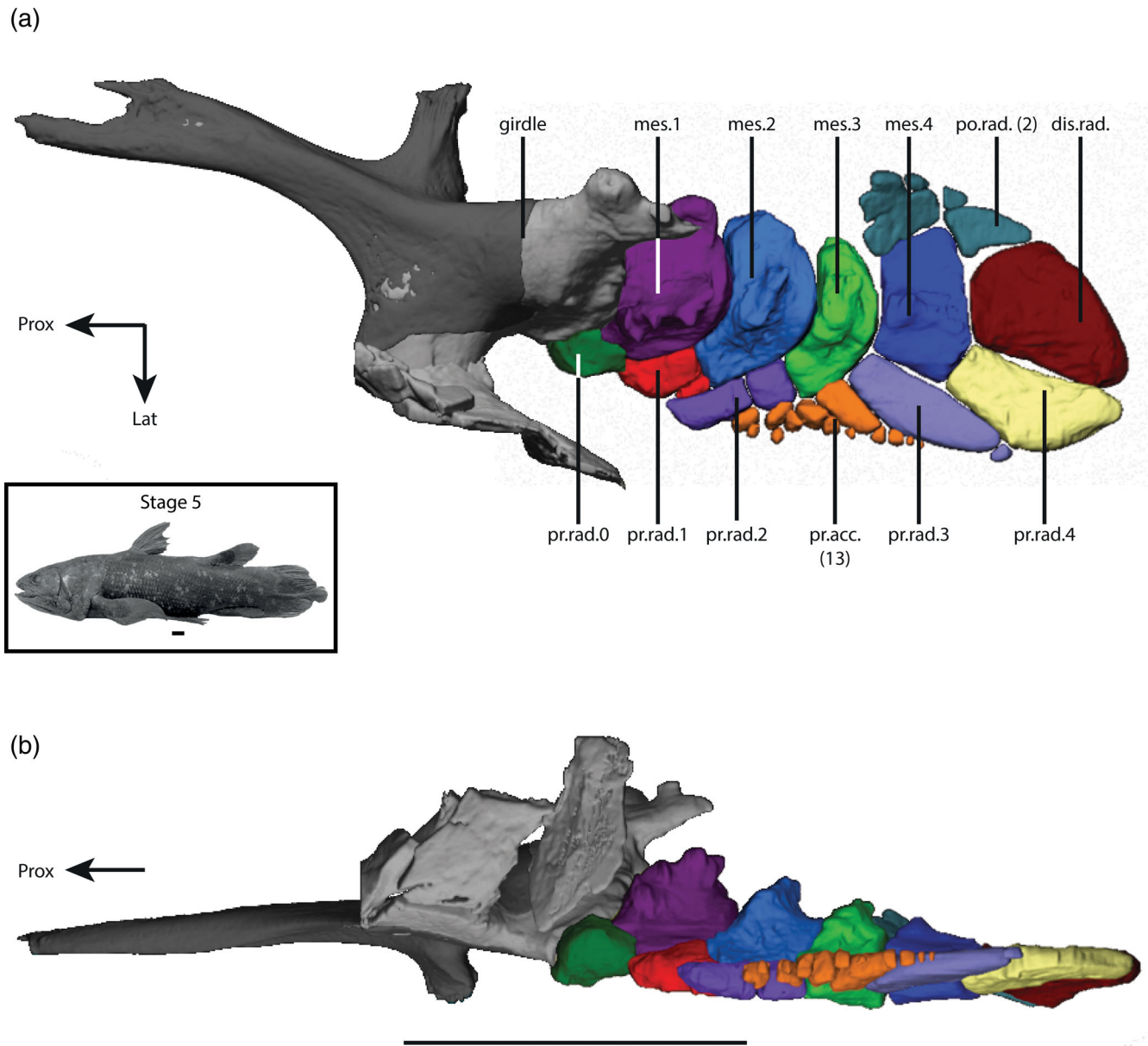
FIGURE 6 *Latimeria chalumnae*—Adult stage. Left pelvic fin in dorsal (a) and lateral (b) view. The lateral process of the girdle is broken. mes., mesomere; po.rad., postaxial radial; pr.acc., preaxial accessory elements; pr.rad., preaxial radial. Scale bar = 50 mm

side of the third mesomere has an important swelling that becomes flatter from pup 2 onward.

3.2.5 | The fourth mesomere (mes.4)

In the adult stage, this mesomere is trapezoid in shape, less wide than the previous mesomeres and without the presence of a medial process (Figure 6). The proximal edge of the mesomere is slightly concave and the distal edge slightly convex, whereas the lateral and medial edges are straight. This mesomere is the only one in contact with the postaxial elements. The medial edge of this mesomere is thinner than the lateral edge. As for the

previous mesomeres, there is a small ridge on the dorsal side of this mesomere. This ridge has a proximo-distal orientation and decreases in height from proximal to distal. This element is not aligned with the previous axial elements but is medially shifted. It is surrounded by the pre-axial radial 3, the preaxial radial 4, the distal radial, and the postaxial radials from its preaxial side (corresponding to its lateral edge) to its postaxial side (corresponding to the medial edge).

In the fetus, the fourth mesomere of the right fin presents an arrowhead-shape, wider than long with a strongly concave proximal edge (Figure 7a). The shape of the left mesomere is elongated, with a slightly concave proximal edge (Figure 10a). From pup 1 onward, the
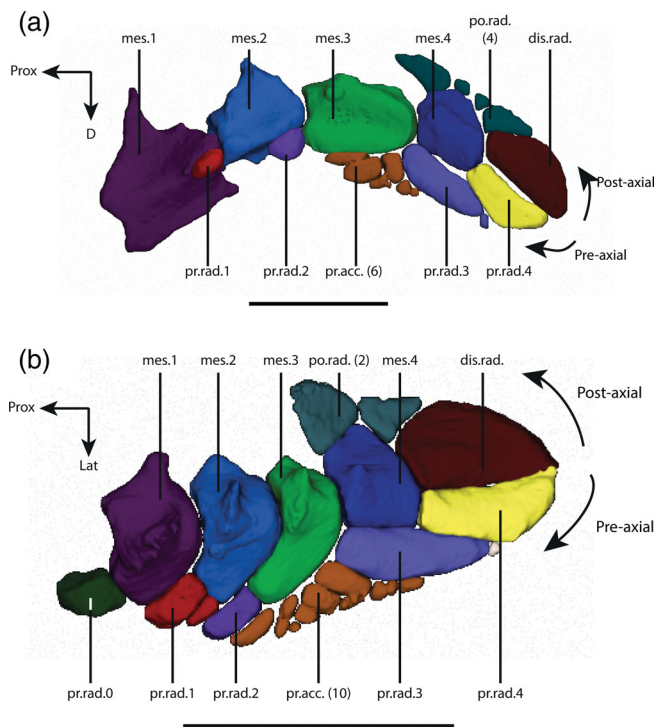
FIGURE 7 *Latimeria chalumnae*—pup 2. Comparison between the left pectoral (a) and pelvic fin (b). The pectoral fin is reversed to have a better comparison with the pelvic fin. The organization of the endoskeletal elements of the pectoral and pelvic fins is the same, except for the presence of the preaxial radial 0 on the pelvic fin. mes., mesomere; po.rad., postaxial radial; pr.acc., preaxial accessory elements; pr.rad., preaxial radial. Scale bar = 10 mm

mesomere has its trapezoidal shape, as in the adult (Figure 7b–e).

3.2.6 | The preaxial elements

The preaxial elements are situated on the lateral edge of the pelvic fin. The organization of the radial elements along the metapterygial axis is similar on the pelvic fin and on the pectoral fin, except for the presence of a preaxial radial (called preaxial radial 0) on the pelvic fin only (Figure 7). As in the pectoral fin (Mansuit et al., 2019; Millot & Anthony, 1958) there is an important difference in morphology of the preaxial radial elements between the most proximal elements (pr.rad. 0–2) and the distal elements (pr.rad. 3–4).

3.2.7 | The preaxial radial 0 (pr.rad.0)

In the adult stage, this element has a square shape and lies in the prolongation of the lateral edge of the first

mesomere. It is in contact with the ventral side of the latero-distal part of the pelvic girdle (Figure 6). The medial articular surface of the preaxial radial 0, in contact with the pelvic girdle, is slightly concave.

In the fetus, this element is rectangular in dorsal view with a triangular section (Figure 7a). From pup 1 onward, this element is square in shape (Figure 7b–e).

3.2.8 | The preaxial radial 1 (pr.rad.1)

In the adult stage, this element forms the prolongation of the lateral edge of the second mesomere and is in contact with the lateral part of the distal edge of the first mesomere (Figure 6). The preaxial radial 1 is formed by two parts, a large and rectangular proximal element and a small distal element with a triangular shape.

In the fetus, this element is single and elongated (Figure 7a). In pup 1, this element is also single and rectangular in shape (Figure 7b). In pup 2, the preaxial radial 1 is fully formed and composed of two elements (Figure 7c–e). In the juvenile, only one element can be reconstructed from the MRI scans but this may be due to the lack of precision in the MRI data (Figure 7d).

3.2.9 | The preaxial radial 2 (pr.rad.2)

In the adult stage, the preaxial radial 2 forms the prolongation of the lateral side of the third mesomere and lies in contact with the lateral part of the distal edge of the second mesomere (Figure 6). The preaxial radial 2 is formed by two elements, a basal square element, adjacent to the mesomere 3, and a rectangular element aligned with the basal element (Figure 7b). This element carries fin rays 1–6 on its dorsal side, whereas it only carries the fin rays 1–4 inserting more distally on its ventral side (Figure 9).

In the fetus, this element does not appear individualized from the mesomere 3. From pup 1 onward, the preaxial radial 2 has its adult shape, with its elongated rectangular shape and the two aligned pieces (Figure 7b). There is some variation in the morphology of this element as in pup 2 and the juvenile specimens preaxial radial 2 only consists of a single elongated element (Figure 7c,d), instead of two aligned elements (Figure 7b,e). However, these observations could be due to the low resolution of the MRI data of the juvenile specimen.

3.2.10 | The preaxial radial 3 (pr.rad.3)

In the adult stage, the preaxial radial 3 is a thin and elongated element, longer than the fourth mesomere,
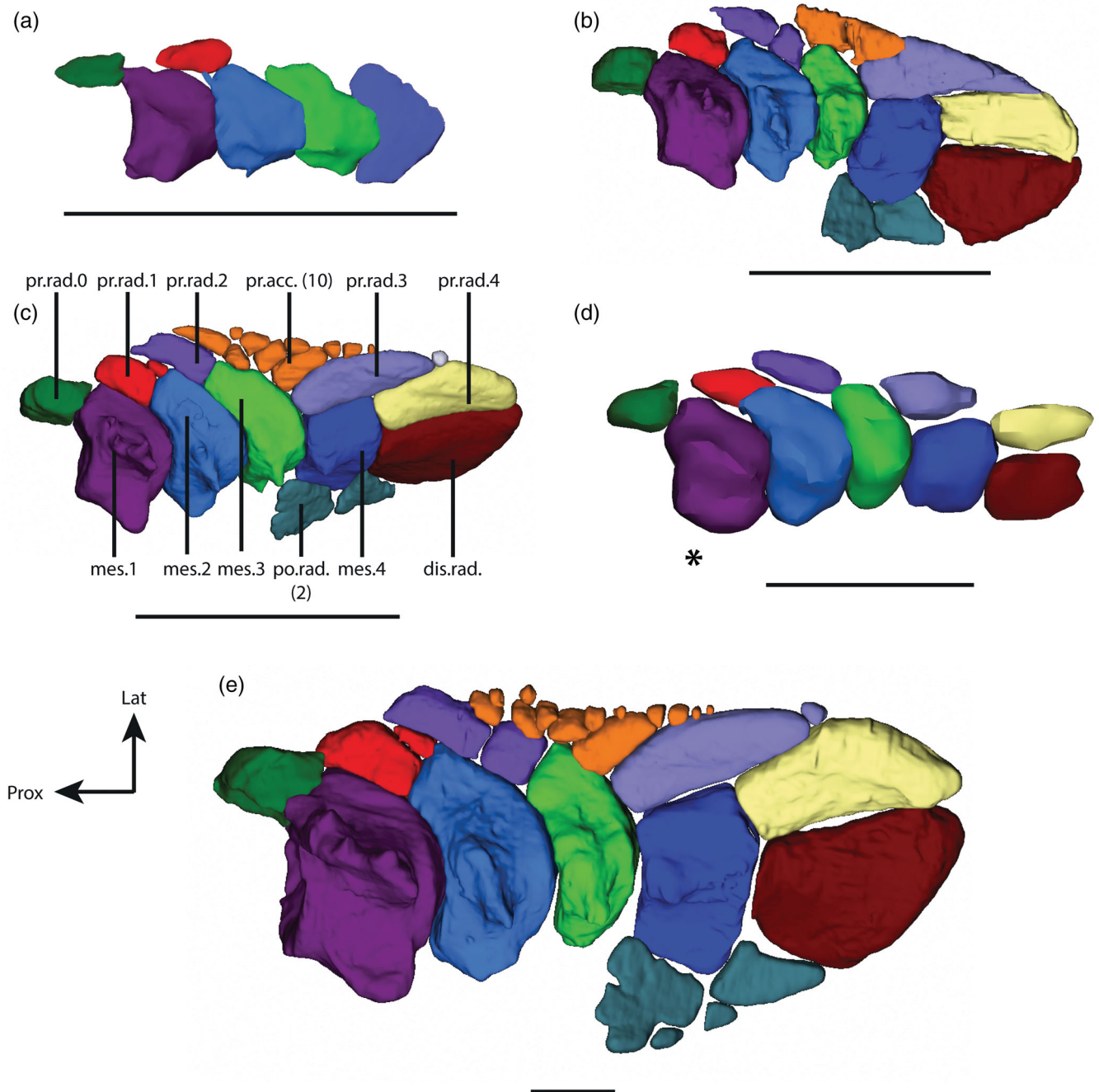
FIGURE 8 *Latimeria chalumnae*. Right (a–d) and left (e - mirror) pelvic fin of five different stages in dorsal view. a: fetus, b: pup 1, c: pup 2, d: juvenile, e: adult. *: The juvenile was scanned using magnetic resonance imaging (MRI) at a low resolution, which did not allow the segmentation of the smallest elements (po.rad., pr.acc.). Corresponding elements of the fin are indicated in the same color. mes., mesomere; po.rad., postaxial radial; pr.acc., preaxial accessory elements; pr.rad., preaxial radial. (a) Scale 2 mm; (b–e) Scale bar = 10 mm

with three straight edges and one distal convex edge (Figure 6). The proximal edge of this element is straight and articulates with the third mesomere. A very small globular element is present at its distal tip. This preaxial radial carries the fin rays 10–13 (Figure 9).

In the fetus, this element is not separated from the fourth mesomere (Figures 7a and 10a). In pup 1, the preaxial radial 3 is thin and elongated, without a separated tip (Figure 7b). Its medial edge is straight and its

latero-distal corner forms a concave angle to fit a preaxial accessory element. This angle could correspond to some elements of preaxial accessory elements that are segmented later in the pup 2 to form the three most distal elements (Figure 7b,c). On the left fin, the distal part of the radial is surrounded by the preaxial radial 4. From pup 2 onward, this element has its adult shape, with an elongated trapezoidal shape and a separated distal small element (Figure 7c–e).
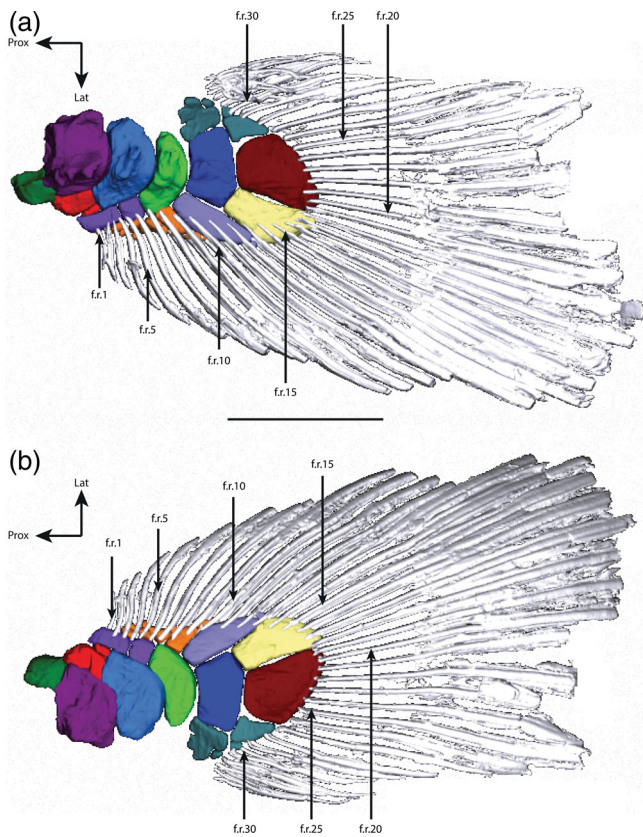
FIGURE 9 *Latimeria chalumnae*—Adult stage. Insertion of the fin rays on the endoskeletal elements of the left fin in dorsal (a) and ventral view (b). The insertion of the fin rays on the preaxial edge of the fin is more proximal on the dorsal edge compared to the ventral edge. f.r., fin ray. Scale bar = 50 mm

3.2.11 | The preaxial radial 4 (pr.rad.4)

The preaxial radial 4, situated at the distal end of the fin endoskeleton, closely resembles the mirror image of the distal radial. As the preaxial radial 3, this element is elongated with three straight edges and a convex distal edge (Figure 6). This element carries the fin rays 14–18 (Figure 9).

In the fetus, the data do not allow the separation of the preaxial radial 4 from the fin rays and muscles on the right fin (Figure 7a), so this element was not segmented. However, it is assumed that the preaxial radial 4 is already present on the right fin. On the left fin, this radial is not separated from the distal radial (Figure 10a). In pup 1, there is a bilateral asymmetry, since the medial edge of the preaxial radial 4 is straight on the right fin (Figure 7b), but concave on the left fin, forming a space between this element and the distal radial (Figure 10b). The lateral edge of the preaxial radial 4 forms an angle that surrounds the distal part of the preaxial radial 3. From pup 2 onward, the preaxial radial 4 has the same trapezoidal shape as described for the adult (Figure 7c–e).
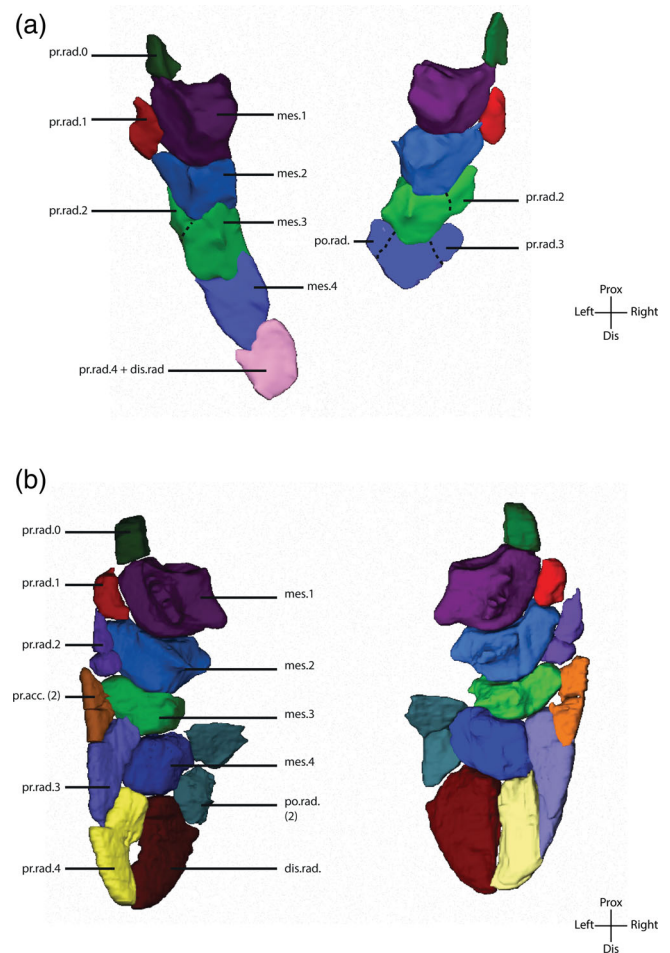

FIGURE 10 *Latimeria chalumnae*—Fetus (a) and pup 1 (b) stages. Right and left pelvic fins in dorsal. Dotted lines show the supposed splitting zone between the mesomere and the preaxial and postaxial elements. (b) There is an asymmetry between the right and left fin in the pup 1 stage, on the distal part of the fin. mes., mesomere; po.rad., postaxial radial; pr.acc., preaxial accessory elements; pr.rad., preaxial radial. Not to scale

3.2.12 | The preaxial accessory elements (pr.acc.)

In the adult stage, these small elements (called "*éléments accessoires de la troisième pièce radiale préaxiale*" by Millot & Anthony, 1958) are positioned in a patch between the distal edges of the third mesomere, the preaxial radial 2, and the lateral edge of the preaxial radial 3 (Figure 6). According to Millot and Anthony (1958), the pelvic fin presents four of these elements at the adult stage. However, both our segmentation of the scan of the pelvic fin and the observation of the isolated fin show a variation in the number of preaxial accessory elements. Indeed, there are 13 elements in adult stage CCC 27 (Figures 6 and 7e), whereas there are at least five accessory elements in the isolated fin of CCC 7. The difference in numbers of elements observed in the different fins can

be explained by the size of the smallest elements, not visible to the naked eyes and hidden by dermal fin rays covering them. The preaxial accessory elements carry the fin rays 7–9 on the dorsal side of the fin and the fin rays 5–9 on the ventral side of the fin (Figure 9).

These elements are not present in the fetus and appear at the pup 1 stage (Figure 7). In the pup 1 stage, there are only two elements, as large as the preaxial radials 2 (Figure 7b). These two elements become fragmented during development since there are at least 10 small elements in pup 2 (Figure 7c) and 13 elements in the adult. In the juvenile, we assume that the preaxial accessory elements are present, but the MRI data did not allow the visualization of the preaxial accessory elements.

3.2.13 | The postaxial elements

3.2.14 | The distal radial (dis.rad.)

In the adult stage, the distal radial is similar in shape to the preaxial radial 4 as a mirror image, although almost twice as wide (Figure 6). It has three more or less straight edges and a convex distal edge. It carries the fin rays 19–27 (Figure 9).

In the fetus, only the left distal radial could be segmented (Figure 10a). We assumed that the right distal radial is also present at this stage, but as for the preaxial radial 4, the data did not allow the separation of this element from the muscles and the fin web. This element is small and square except for its proximal edge that is slightly concave. In pup 1, the left fin presents an ovoid space between the distal radial and the preaxial radial 4 (Figure 10b). Such a space is not present on the right fin (Figure 7b). Its medial edge forms an angle that surrounds the postaxial radials in the left fin. From pup 2 onward, the distal radial is fully formed with the trapezoidal shape observed in the adult stage (Figure 7c–e). According to Millot and Anthony (1958) there is a longitudinal ridge on the dorsal side of this element, but such a ridge does not appear on the 3D modeling or on the observed isolated pelvic fin.

3.2.15 | The postaxial radials (po.rad.)

The postaxial radials are located at the medial edge of the pelvic fin in articulation with the fourth mesomere and the distal radial. In the adult stage, Millot and Anthony (1958) described three elements among the postaxial radials. The proximal element presents a large triangular shape and is located on the medial edge of the fourth mesomere. On the left fin of CCC 27, this element is split into a large piece and a small one (Figure 6), whereas there is only one proximal element on the right fin, as is observed for the isolated prepared fin of CCC 7 and as described by Millot and Anthony (1958). The distal element is slightly smaller, with a quadrangular shape and located on the medial part of the distal edge of the fourth mesomere and on the medial edge of the distal radial (Figure 6). The third element is very small compared to the other postaxial radials, triangular-shaped, and located between the proximal and the distal one. The postaxial radials carry the fin rays 28–34 (Figure 9).

In the fetus, these elements cannot be individually identified or separated from the mesomere 4 in the right fin (Figures 7a and 10). In the pup 1 and pup 2 the postaxial radials are well developed, but with only two elements (Figure 7b,c).

3.2.16 | The fin rays

The pelvic fin in the adult stage presents 37 fin rays (Figure 9), which are numbered 1 from the preaxial (lateral) to 37 at postaxial (medial) side of the fin. As for the pectoral fin, the proximal part of each fin ray is bifurcated, one branch inserting on the dorsal face of the fin and one branch inserts on the ventral face of the fin. The first ray is very small, and the next rays become longer along the preaxial side of the fin, up to the axis of the fin, to progressively decrease in size along the postaxial side of the fin. As for the pectoral fin, the rays of the preaxial side of the fin insert largely on the preaxial elements, whereas the rays on the postaxial side of the fin insert only on the medial edges of the distal radial and the postaxial radials. The three last fin rays 35–37 are free and do not insert on fin elements. The fins rays are inserted more proximally on the dorsal than on the ventral side on the preaxial side of the fin.

4 | DISCUSSION

As discussed in our previous study (Mansuit et al., 2019), even if the gestation time for coelacanths is estimated at more to 13 months (Hureau & Ozouf, 1977), it is not possible to precisely determine the time between the different stages.

4.1 | Morphology of the pelvic girdle

Unlike the pectoral girdle, the pelvic girdle is only formed by a unique endoskeletal bone as described by Millot and Anthony (1958). Unlike in lungfishes as *Neoceratodus* (Boisvert et al., 2013) the two hemi-girdles are not fused (Figure 4c) but only linked by ligaments

(Millot & Anthony, 1958). The general shape of the pelvic girdle of *Latimeria chalumnae* is similar to what is observed in fossil coelacanths with an anterior rod-like process, a lateral and a medial processes (Forey, 1998). According to Forey (1998), the lateral process corresponds to the ilium (*iliac process* of Coates & Ruta, 2007), the medial process to the ischium (*ischial process* of Coates & Ruta, 2007), and the anterior process to the pubis of the pelvic girdle of tetrapods. However, the homology between the lateral and medial processes with the *ilium* and *ischium* remains uncertain (Ahlberg, 1989). Therefore, we preferred to use the neutral terminology proposed by Millot and Anthony (1958) (i.e., *medial* and *lateral processes*, and *anterior process*) to avoid any ambiguities regarding the homology of these structures. In extant tetrapods, the ilium, ischium, and pubis are formed through different ossification centers (Malashichev, 2001; Maxwell & Larsson, 2009; Rocková & Rocek, 2005). In the extant coelacanth *Latimeria*, as in lungfish (Schultze, 1986) the girdle is cartilaginous (Millot & Anthony, 1958) and there is only an ossification of the anterior part of the girdle and medial process, but not for the lateral process (Figures 2e–4). Moreover, the ossification of the pelvic girdle begins at the anterior process of the girdle, subsequently extending to the medial process of the girdle (Figure 5). Consequently, only a single ossification center appears to be present in the pelvic girdle of *Latimeria*. Only based on anatomical observations, it is thus not possible to assign a homology to the different parts of the girdle in *Latimeria* relative to the different bones of the girdle of tetrapods.

The anterior process/blade of the pelvic girdle seems to be common in actinopterygian fishes (e.g., Andrews & Westoll, 1970; Faustino & Power, 1999; Grandel & Schulte-Merker, 1998; Yamanoue, Setiamarga, & Matsuura, 2010) and sarcopterygian fishes (Andrews & Westoll, 1970; Boisvert et al., 2013; Forey, 1998). According to Andrews and Westoll (1970), this anterior process forms an insertion area for abdominal muscles and ligaments. In *Latimeria*, however, only the extremity of this process supports the abdominal muscles. The main part of the blade forms the attachment site for the pelvic fin muscles (Millot & Anthony, 1958) (personal observations).

As for the articular head of the pectoral girdle (Millot & Anthony, 1958), the acetabulum of the pelvic girdle of *Latimeria* is convex. This convex articular surface is a feature shared by coelacanths and dipnomorphs (Boisvert et al., 2013; Shubin, 1995). In tetrapodomorphs, the pelvic girdle shows a concave acetabulum, where the first mesomere fits (Ahlberg, 1989; Boisvert et al., 2013; Shubin, 1995). A concave acetabulum was considered as the primitive condition for sarcopterygians (Ahlberg, 1989), and the convex acetabulum of coelacanths and

dipnomorphs as a derived character. Even if the precise interrelationships of sarcopterygians remain debated, the current consensus presents coelacanths as sister-taxa of tetrapods and lungfishes (e.g., Ahlberg, 1991; Amemiya et al., 2013; Cloutier & Ahlberg, 1996; Friedman et al., 2007). It thus appears that a convex acetabulum is the primitive condition for sarcopterygians.

The micro-tomographic imaging highlights, for the first time, the presence of a dense surface around part of the pelvic girdle, and the presence of a dense trabecular system within the girdle (Figure 4b). The pelvic girdle of *Latimeria* is cartilaginous (Forey, 1998; Millot & Anthony, 1958), and this dense surface and the trabecular system might be an endochondral ossification of the girdle. The presence of a trabecular system in the pelvic girdle of *Latimeria* might reinforce its structural resistance when loaded by pelvic muscle forces. Indeed, many *levator* and *depressor* muscles of the pelvic fin insert on the anterior part of the girdle and on the medial process (Millot & Anthony, 1958) (personal observations). In tetrapods, it has been shown that the ossification of the bones is influenced by muscular activity during the embryonic development (Boisvert et al., 2013; Hall, 1986; Newman & Müller, 2005). It is therefore likely that the same process occurs in *Latimeria* where the young develop in the mother and likely show muscular contractions before birth. The ossification of the bone occurs only from the pup 1 stage. Forey (1998) noted that the pelvic girdle of extinct coelacanths often presents an open concave posterior end, and that the acetabulum is missing. It could be assumed that only the ossified part of the pelvic girdle is preserved in the fossil record, and that the cartilaginous posterior part of the girdle does not fossilize. The trabecular system highlighted in *Latimeria* has never been described in the fossil records for coelacanths and other osteichthyan fishes, and remains to be determined whether this feature is specific to *Latimeria* or if other bony fishes possess a trabecular system in the pelvic girdle.

4.2 | Morphology of the pelvic fin

In *Latimeria*, the general organization of the pelvic fin endoskeleton is similar to that of the pectoral fin (Millot & Anthony, 1958; Panchen & Smithson, 1990), particularly the distal part of the fin (pr.rad. 3–4, pr.acc., dis.rad., po. rad.) (Figure 7). This endoskeletal morphology of the pectoral and pelvic fins/limbs is shared by all sarcopterygians (Rosen, Forey, Gardiner, & Patterson, 1981). In all crown-sarcopterygians, these paired appendages are connected to their respective girdle via a mono-basal articulation (Clack, 2012; Janvier, 1996; Rosen et al., 1981), whereas stem-sarcopterygians are assumed to have a poly-basal fin articulation (Zhu & Yu, 2009). In *Latimeria* and in other

sarcopterygian fishes, the pelvic fin is smaller than the pectoral one (e.g., Ahlberg, 1989; Andrews & Westoll, 1970; Boisvert, 2005; Forey, 1998; Jeffery, Storrs, Holland, Tabin, & Ahlberg, 2018). The major difference between the pelvic and pectoral fins, in *Latimeria*, lies in the presence of a preaxial radial 0, which articulates with the pelvic girdle and the first mesomere (Figure 7b). This element is absent in the pectoral fin (Figure 7a). The preaxial radial 0 was previously described (Millot & Anthony, 1958) and is also present in the pelvic fin of the Triassic coelacanth *Laugia groenlandica* (Stensiö, 1932) (specimen NHMD 152716, personal observation), but never received developmental or phylogenetic consideration. Indeed, the presence of this small element questions the mono-basal condition of the pelvic fin of *Latimeria* and coelacanths in general, and may question the synapomorphy of crown-sarcopterygians [a mono-basal articulation of paired fins (Janvier, 1996; Rosen et al., 1981; Zhu & Yu, 2009)]. The development of the pelvic fin suggests that the presence of this element in contact with the girdle is due to the particular morphology of the mesomeres. This element may correspond to the preaxial radial 1 of the pectoral girdle (see below). Thus, the pluri-basal condition of the pelvic fin of *Latimeria* would be a specificity of coelacanths.

Although the general organization of the endoskeleton of the pelvic and pectoral fins is similar, some differences can be observed (Figure 6). The mesomeres of the pectoral fin are longer than wide, with a quadrangular shape (Mansuit et al., 2019; Millot & Anthony, 1958). By contrast, the mesomeres of the pelvic fin are shorter than wide with an arc shape, dorsoventrally flattened, with a ridge on their dorsal side. These differences between the shape of the mesomeres of the pelvic and pectoral fins appear to be also present in the Triassic coelacanth *Laugia groenlandica* (Stensiö, 1932) (personal observations).

There are marked differences in the size and shape of the most proximal radial elements between the pectoral and pelvic fins. The preaxial radials 1–2 of the pectoral fin are small compared to the mesomeres, ovoid in shape, and in contact with the distal part of the associated mesomere (Figure 7a). By contrast, the preaxial radials 1–2 of the pelvic fin are proportionally larger and in contact with both the associated and the following mesomeres (Figures 6 and 7b). In the fossil tetrapodomorph fishes *Eusthenopteron* and *Panderichthys*, the preaxial radials 1–2 of the pelvic fin have a similar shape, although slightly smaller, than those of the pectoral fin (Andrews & Westoll, 1970; Boisvert, 2005). Their morphology is different from that of *Latimeria*: they are elongated elements that articulate with the distal edge of the associated mesomere, and more or less parallel to the long edge of the following mesomere.

According to Forey (1998), the pelvic fin of *Latimeria* presents an important degree of asymmetry to the central axis compared to the pectoral fin, that is, the organization and arrangement of the elements are different between the preaxial and the postaxial edge of the fin. As for the pectoral fin (Mansuit et al., 2019; Millot & Anthony, 1958), the arrangement of the pre-axial and postaxial elements along the metapterygial axis of the pelvic fin of *Latimeria* is asymmetrical. The mesomeres of the pelvic fin are all associated with preaxial radials, whereas only the fourth mesomere is associated with postaxial elements (postaxial radials and distal radial). Moreover, the presence of the preaxial radial 0 on the pelvic fin, not present on the pectoral fin, increases the asymmetry to the central axis of the pelvic fin. However, as for the pectoral fin, the most proximal preaxial radials (0–2) of the pelvic fin are small and globular or rectangular shape, whereas the distal preaxial radials (3–4) are thin and elongate (Millot & Anthony, 1958) (Figure 6). This difference of shape is related to muscle insertions. Indeed, some muscles insert on the preaxial radials 0–2, whereas for the preaxial radial 3–4, the muscles inserted at the base of the fin rays that are associated with the radials (Mansuit et al., in prep.). Considering the general endoskeletal arrangement, the pelvic fin of *Latimeria* shows a short lobe-shaped silhouette compared to that of the more elongate lobed pectoral fin. The insertion of the fin rays on the fin is also more asymmetrical on the pelvic fin compared to the pectoral fin (Friedman et al., 2007; Millot & Anthony, 1958). Fin rays of the pelvic fin insert more proximally on the preaxial side than on the postaxial side (Figure 9) compared to the pectoral fin where the fin web shows a more symmetrical arrangement around the metapterygial axis. However, as for the pectoral fin, the most proximal preaxial radials (preaxial radial 0–1) are not associated with the pelvic fin rays. An asymmetrical arrangement of the pelvic fin rays along the metapterygial axis has also been suggested in the Triassic coelacanth *Laugia groenlandica* (Forey, 1998; Stensiö, 1932). An asymmetry is also present on the fin ray arrangements between the dorsal and ventral sides of the pelvic fin. Indeed, the fin rays insert more proximally on the dorsal side of the fin than on the ventral side (Figure 9). This asymmetrical coverage of the paired fin rays is also shared by the fossil coelacanths *Laugia groenlandica* (Forey, 1998; Stensiö, 1932), the extant lungfish *Neoceratodus* and fossil tetrapodomorph fishes, such as *Eusthenopteron* and *Tiktaalik* (Stewart et al., 2019).

4.3 | Development of the pelvic appendage

The most pronounced changes in the pelvic girdle morphology occur between the fetus and pup 1, and notably

entail the elongation of the anterior part of the girdle (Figure 5a,b). The elongation of the girdle during the development seems to be common in osteichthyan fishes, since it is observed both in actinopterygians, for example in *Pagrus major* (Matsuoka, 1985), *Chanos chanos* (Taki, Kohno, & Hara, 1986), *Danio rerio* (Grandel & Schulte-Merker, 1998), and *Sparus aurata* (Faustino & Power, 1999), and in the lungfish *Neoceratodus forsteri* (Boisvert et al., 2013). However, the pelvic girdle mainly grows in a posterior direction in the axolotl *Ambystoma mexicanum* (Boisvert et al., 2013), whereas the pubis has a small anterior growth.

Although very similar, the development of the pelvic fin appears to lag behind that of the pectoral fin in *Latimeria*. The assumption of a delay in the development of the pelvic appendage is based on the morphology of the endoskeletal elements observed in the fetus. At this stage, all mesomeres of the pectoral fin are formed, and the radial elements are present, at least as cartilaginous plates. However, most of the radial elements are not differentiated from the mesomere 4 and the distal radial in the pelvic fin (Figures 8 and 10a), which suggests that its development is delayed compared to the pectoral fin. A delay in the development of the pectoral and pelvic appendages is also observed in chondrichthyans (Ballard, Mellinger, & Lechenault, 1993; Didier, Leclair, & Vanbuskirk, 1998; Ziermann, Freitas, & Diogo, 2017), actinopterygians (Faustino & Power, 1999; Grandel & Schulte-Merker, 1998), and sarcopterygians (Boisvert et al., 2013; Joss & Longhurst, 2001). Therefore, *Latimeria* likely follows the general gnathostome pattern of paired appendages development. In the *Latimeria* fetus, only the most proximal preaxial radials (pr.rad. 0–1) are present in the pelvic fin (Figure 8). However, from pup 1 stage onward all the elements of the fin are present. Contrary to what is observed during the development of the pectoral fin (Mansuit et al., 2019), there is no cartilaginous plate around the metapterygial axis of the pelvic fin.

Based on the comparison of the morphology of the mesomeres during the development, we suggest a developmental mechanism for the endoskeletal elements of the pelvic fin. Along the preaxial edge of the fin, the distribution of the radials matches that of the mesomeres (e.g., mes.1 and pr.rad.0) in the pups and adult. In the fetus, only the radials 0 and 1 are present. In addition, the mesomere 3 presents a general shape that is different from that observed in later stages, with the presence of a well-developed proximo-lateral extension (Figures 8 and 10a). Similarly, the mesomere 4 (observed in the right pelvic fin), which is the most distal endoskeletal element in the fetus fin, has an arrowhead shape with lateral and medial extensions around the distal end of the mesomere 3. These lateral extensions of the mesomeres 3 and 4 are lost in later developmental stages (Figure 8), while there

is a progressive increase in the number of elements on the preaxial side of the fin. An additional preaxial radial and two preaxial accessory elements are observed in pup 1, and the number of preaxial accessory elements increases in pup 2 (10) and in the adult (13) (Figure 8). This pattern suggests that the preaxial radials are formed through the fragmentation of the radial extension of the adjacent mesomere, following a proximo-distal sequence during the development (i.e., the first mesomere splits first). In this scenario, the extension of mesomere 3 observed in the fetus gives rise to the preaxial radial 2 in the pup. From pup 1 onward, a series of preaxial and postaxial radials surrounds the mesomere 4. We suggest that these elements derive, respectively, from the lateral and medial extensions of the mesomere 4 observed in the fetus. The distal end of the left fin is formed by a distal plate in the fetus, which might correspond to the distal radial and the preaxial radial 4 from pup 1 onward (Figure 10). Yet, additional developmental stages are needed to better understand the origin of the distal elements of the pelvic fin, such as the preaxial radial 3, and the potential contribution of the mesomere 4 and distal plate in the formation of these elements.

The formation of the preaxial radials is not clearly understood in the extant lungfish *Neoceratodus*. Previous studies suggest two different patterns of development to explain their formation. In the first scenario, the radials arise de novo process (Joss & Longhurst, 2001): they are formed by a distinct mesenchymal condensation and are unconnected to other elements (Johanson et al., 2007; Shubin & Alberch, 1986). In the second scenario, the radials arise from the fragmentation of the associated mesomere (Joss & Longhurst, 2001), i.e., the element is formed by a continuous plate of precartilage that subsequently breaks up into two separate elements (Shubin & Alberch, 1986). This second scenario could corroborate our hypothesis of the splitting of the mesomere. However, we suggested previously that the preaxial radials are formed by the fragmentation of the following mesomeres, and not the associated mesomeres as in *Neoceratodus*. Since the mesomeres of the pelvic fin of *Latimeria* have an arc-shape it is possible that the position of the preaxial radials is different compared to that observed for the pectoral fin. If so, this would suggest that the preaxial radial 0 of the pelvic fin corresponds to the preaxial radial 1 of the pectoral fin (and the pr.rad.1 of the pelvic fin to the pr.rad.2 of the pectoral fin). The preaxial radial 3 of the pelvic fin would then not correspond to any preaxial radial in the pectoral fin, and this element could have been lost in the pectoral fin. If there is a correspondence between pectoral and pelvic preaxial radials, the polybasal condition of the pelvic fin in *Latimeria* may be a derived character in sarcopterygians due to the shape of

the mesomeres. Concerning the formation of the postax-ial elements, these elements are supposed to arise de novo in *Neoceratodus* (Johanson et al., 2007; Joss & Longhurst, 2001), but a fragmentation process cannot be excluded in *Latimeria*, as explained above.

5 | CONCLUSION

As in other vertebrates, the development of the pelvic fin occurs later than that of the pectoral fin in *Latimeria*: many elements of the endoskeleton are not formed yet in the earliest stage sampled here. In the fetus, only the four mesomeres and the most proximal radial elements (pre-axial radial 0–1) are formed. The mesomeres 3 and 4 show prominent extensions in the fetus but not in later stages. We suggest that the radial elements (preaxial radials 0–4, preaxial accessory elements, and postaxial radials) origi-nate from the fragmentation of the mesomeres (e.g., pr. rad.0 fragments from mes. 1). Since the pectoral and pel-vic fins show a similar organization of their endoskeleton and development, it is most probable that the same mechanism underpins the formation of both paired fins. The progressive ossification of the pelvic girdle and the formation of a trabecular system in the adult stage are documented here. This trabecular system might rein-force the cartilaginous girdle to withstand the muscle forces exerted during locomotion. However, it remains unknown whether this trabecular system is unique to *Latimeria chalumnae* or shared by other extinct coela-canths or early sarcopterygians. Finally, the presence of a preaxial element in contact with the pelvic girdle from the earliest stage of development onward questions the mono-basal condition of the pelvic fin in *Latimeria*. The presence of this element raises questions a synapomor-phy of crown-sarcopterygians: the mono-basal articula-tion of paired fins. But the particular shape of the mesomeres of the pelvic fin and the process of develop-ment of preaxial radials may explain the presence of this element in contact with the girdle. This element could be homologous to the preaxial radial 1 on the pectoral fin.

AUTHOR CONTRIBUTIONS
Rohan Mansuit: Conceptualization; data curation; formal analysis; methodology; software; writing-original draft. **Gaël Clément:** Conceptualization; data curation; formal analysis; funding acquisition; supervision; valida-tion; writing-review and editing. **Anthony Herrel:** Con-ceptualization; data curation; formal analysis; funding acquisition; supervision; validation; writing-review and editing. **Hugo Dutel:** Formal analysis; methodology; software; validation; writing-review and editing. **Paul Tafforeau:** Formal analysis; methodology; software; validation; writing-review and editing. **Mathieu Santin:** Formal analysis; methodology; software; validation; writing-review and editing. **Marc Herbin:** Conceptuali-zation; data curation; formal analysis; funding acquisi-tion; supervision; validation; writing-review and editing.

DATA AVAILABILITY STATEMENT
The synchrotron data will be available on the ESRF data-base, at the following address: http://paleo.esrf.fr/ (fetus, pup1, pup2, juvenile). The CT-scan data are available at the following address: http://coldb.mnhn.fr/catalognumber/mnhn/za/ac-2012-21 (adult). The MRI data will be avail-able at the following address: https://www.morphosource.org/ (juvenile). All the data are also available by request from the authors.

ORCID
Rohan Mansuit 🔘 https://orcid.org/0000-0002-4727-3650
Anthony Herrel 🔘 https://orcid.org/0000-0003-0991-4434
Hugo Dutel 🔘 https://orcid.org/0000-0002-1908-5150
Paul Tafforeau 🔘 https://orcid.org/0000-0002-5962-1683
Mathieu D. Santin 🔘 https://orcid.org/0000-0003-4251-0538

REFERENCES
Ahlberg, P. E. (1989). Paired fin skeletons and relationships of the fossil group Porolepiformes (Osteichthyes: Sarcopterygii). *Zoo-logical Journal of the Linnean Society*, *96*, 119–166.
Ahlberg, P. E. (1991). A re-examination of sarcopterygian interrela-tionships, with special reference to the Porolepiformes. *Zoologi-cal Journal of the Linnean Society*, *103*, 241–287.

Amemiya, C. T., Alfoldi, J., Lee, A. P., Fan, S., Philippe, H., MacCallum, I., ... Lindblad-Toh, K. (2013). The African coelacanth genome provides insights into tetrapod evolution. *Nature*, *496*, 311–316.

Andrews, S. M., & Westoll, T. S. (1970). The postcranial skeleton of *Eusthenopteron foordi* Whiteaves. *Earth and Environmental Science Transactions of the Royal Society of Edinburgh*, *68*, 207–329.

Ballard, W. W., Mellinger, J., & Lechenault, H. (1993). A series of stages for development of *Scyliorhinus canicula* the lesser spotted dogfish (Chondrichthyes: Scyliorhinidae). *Journal of Experimental Zoology*, *267*, 1–43.

Boisvert, C. A. (2005). The pelvic fin and girdle of *Panderichthys* and the origin of tetrapod locomotion. *Nature*, *438*, 1145–1147.

Boisvert, C. A., Joss, J. M., & Ahlberg, P. E. (2013). Comparative pelvic development of the axolotl (*Ambystoma mexicanum*) and the Australian lungfish (*Neoceratodus forsteri*): Conservation and innovation across the fish-tetrapod transition. *EvoDevo*, *4*, 1–19.

Clack, J. A. (2012). *Gaining ground: The origin an evolution of Tetrapods* (pp. 1–523). Bloomington: Indiana University Press.

Cloutier, R., & Ahlberg, P. E. (1996). Morphology, characters, and the interrelationships of basal sarcopterygians. In *Interrelationships of Fishes* (pp. 445–479). NY: Academic Press.

Coates, M. I., & Ruta, M. (2007). Skeletal changes in the transition from fins to limbs. In *Fins into limbs - Evolution, development, and transformation* (pp. 15–38). Chicago: The University of Chicago Press.

Cubbage, C. C., & Mabee, P. M. (1996). Development of the cranium and paird fins in the zebrafish *Danio rerio* (Ostariophysi, Cyprinidae). *Journal of Morphology*, *229*, 121–160.

Cupello, C., Brito, P. M., Herbin, M., Meunier, F. J., Janvier, P., Dutel, H., & Clément, G. (2015). Allometric growth in the extant coelacanth lung during ontogenetic development. *Nature Communications*, *6*, 1–5.

Didier, D. A., Leclair, E. E., & Vanbuskirk, D. R. (1998). Embryonic staging and external features of development of the chimaeroid fish, *Callorhinchus milii* (Holocephali, Callorhinchidae). *Journal of Morphology*, *236*, 25–47.

Dutel, H., Galland, M., Tafforeau, P., Long, J. A., Fagan, M. J., Janvier, P., ... Herbin, M. (2019). Neurocranial development of the coelacanth and the evolution of the sarcopterygian head. *Nature*, *569*, 556–559.

Faustino, M., & Power, D. M. (1999). Development of the pectoral, pelvic, dorsal and anal fins in cultured sea bream. *Journal of Fish Biology*, *54*, 1094–1110.

Forey, P. L. (1998). *History of the coelacanth fishes* (pp. 1–419). London: Chapman & Hall.

Friedman, M., Coates, M. I., & Anderson, P. (2007). First discovery of a primitive coelacanth fin fills a major gap in the evolution of lobed fins and limbs. *Evolution and Development*, *9*, 329–337.

Grandel, H., & Schulte-Merker, S. (1998). The development of the paired fins in the zebrafish (*Danio rerio*). *Mechanisms of Development*, *79*, 99–120.

Hall, B. K. (1986). The role of movement and tissue interactions in the development and growth of bone and secondary cartilage in the clavicle of the embryonic chick. *Journal of Embryology and Experimental Morphology*, *93*, 133–152.

Hureau, J.-C., & Ozouf, C. (1977). Détermination de l'âge et croissance du coelacanthe Latimeria chalumnae Smith, 1939 (Poisson, crossopterygien, Coelacanthidae). *Cybium*, *2*, 129–137.

Janvier, P. (1996). *Early vertebrates* (pp. 1–393). Oxford: Clarendon Press.

Jarvik, E. (1980). *Basic structure and evolution of vertebrates* (pp. 1–575). New York: Academic Press.

Jeffery, J. E., Storrs, G. W., Holland, T., Tabin, C. J., & Ahlberg, P. E. (2018). Unique pelvic fin in a tetrapod-like fossil fish, and the evolution of limb patterning. *Proceedings of the National Academy of Sciences*, *115*, 201810845.

Johanson, Z., Joss, J., Boisvert, C. A., Ericsson, R., Sujita, M., & Ahlberg, P. E. (2007). Fish fingers: Digit homologues in sarcopterygian fish fins. *Journal of Experimental Zoology, Part B: Molecular and Developmental Evolution*, *308*, 757–768.

Joss, J. M., & Longhurst, T. (2001). Lungfish paired fins. In P. E. Ahlberg (Ed.), *Major events in early vertebrate evolution* (pp. 289–306). London: Taylor & Francis.

Jude, E., Johanson, Z., Kearsley, A., & Friedman, M. (2014). Early evolution of the lungfish pectoral-fin endoskeleton: Evidence from the middle Devonian (Givetian) *Pentlandia macroptera*. *Frontiers in Earth Science*, *2*, 1–15.

Lyckegaard, A., Johnson, G., & Tafforeau, P. (2011). Correction of ring artifacts in X-ray tomographic images. *International Journal of Tomography & Simulation*, *18*, 1–9.

Mabee, P. M., & Noordsy, M. (2004). Development of the paired fins in the paddlefish, *Polyodon spathula*. *Journal of Morphology*, *261*, 334–344.

Mabee, P. M., & Trendler, T. A. (1996). Development of the cranium and paired fins in *Betta splendens* (Teleostei: Percomorpha): Intraspecific variation and interspecific comparisons. *Journal of Morphology*, *227*, 249–287.

Malashichev, Y. B. (2001). Sacrum and pelvic girdle development in Lacertidae. *Russian Journal of Herpetology*, *8*, 1–16.

Mansuit, R., Clément, G., Herrel, A., Dutel, H., Tafforeau, P., Santin, M. D., & Herbin, M. (2019). Development and growth of the pectoral girdle and fin skeleton in the extant coelacanth *Latimeria chalumnae*. *Journal of Anatomy*, *236*, 493–509.

Matsuoka, M. (1985). Osteological development in the red sea bream, *Pagrus major*. *Japanese Journal of Ichthyology*, *32*, 35–51.

Maxwell, E. E., & Larsson, H. C. E. (2009). Comparative ossification sequence and skeletal development of the postcranium of palaeognathous birds (Aves: Palaeognathae). *Zoological Journal of the Linnean Society*, *157*, 169–196.

Millot, J., & Anthony, J. (1958). *Anatomie de Latimeria Chalumnae, Tome I : Squelette, Muscles et Formations de Soutien* (pp. 1–122). Paris: CNRS.

Millot, J., & Anthony, J. (1965). *Anatomie de Latimeria Chalumnae, Tome II : Système Nerveux et Organes Des Sens* (pp. 1–130). Paris: CNRS.

Millot, J., Anthony, J., & Robineau, D. (1978). *Anatomie de Latimeria Chalumnae, Tome III: Appareil Digestif, Appareil Respiratoire, Appareil Urogenital Glandes Endocrines, Appareil Circulatoire Téguments, Ecailles, Conclusions Générale* (pp. 1–198). Paris: CNRS.

Newman, S. A., & Müller, G. B. (2005). Origination and innovation in the vertebrate limb skeleton: An epigenetic perspective. *Journal of Experimental Zoology, Part B: Molecular and Developmental Evolution*, *304*, 593–609.

Nulens, R., Scott, L., & Herbin, M. (2011). *An updated inventory of all known specimens of the coelacanth, Latimeria spp* (Vol. 3,

pp. 1–52). Grahamstown, South Africa: Smithiana Publications in Aquatic Biodiversity.

Paganin, D., Mayo, S. C., Gureyev, T. E., Miller, P. R., & Wilkins, S. W. (2002). Simultaneous phase and amplitude extraction from a single defocused image of a homogeneous object. _Journal of Microscopy_, _206_, 33–40.

Panchen, A. L., & Smithson, T. R. (1990). The pelvic girdle and hind limb of _Crassigyrinus scoticus_ (Lydekker) from the Scottish carboniferous and the origin of the tetrapod pelvic skeleton. _Transactions of the Royal Society of Edinburgh: Earth Sciences_, _81_, 31–44.

Pouyaud, L., Wirjoatmodjo, S., Rachmatika, I., Tjakrawidjaja, A., Hadiaty, R., & Hadie, W. (1999). A new species of coelacanth. _Life Sciences_, _322_, 261–267.

Rocková, H., & Rocek, Z. (2005). Development of the pelvis and posterior part of the vertebral column in the Anura. _Journal of Anatomy_, _206_, 17–35.

Rosen, D. E., Forey, P. L., Gardiner, B. G., & Patterson, C. (1981). Lungfishes, tetrapods, paleontology, and plesiomorphy. _Bulletin of the American Museum of Natural History_, _167_, 159–276.

Sanchez, S., Ahlberg, P. E., Trinajstic, K. M., Mirone, A., & Tafforeau, P. (2012). Three-dimensional synchrotron virtual paleohistology: A new insight into the world of fossil bone microstructures. _Microscopy and Microanalysis_, _18_, 1095–1105.

Schultze, H.-P. (1986). Dipnoans as sarcopterygians. _Journal of Morphology_, _190_, 39–74.

Shubin, N. H. (1995). The evolution of paired fins and the origin of tetrapod limbs. In _Evolutionary biology_ (pp. 39–86). Boston: Springer.

Shubin, N. H., & Alberch, P. (1986). A morphogenetic approach to the origin and basic organization of the tetrapod limb. _Evolutionary Biology_, _20_, 319–387.

Smith, J. L. B. (1939). A living fish of Mesozoic type. _Nature_, _143_, 455–456.

Stensiö, E. A. (1932). Triassic fishes from East Greenland: Collected by the Danish expeditions in 1929-1931. _Meddelelser Om Greenland_, _83_, 1–305.

Stewart, T. A., Lemberg, J. B., Taft, N. K., Yoo, I., Daeschler, E. B., & Shubin, N. H. (2019). Fin ray patterns at the fin-to-limb transition. _Proceedings of the National Academy of Sciences_, _117_(3), 1612–1620.

Taki, Y., Kohno, H., & Hara, S. (1986). Early development of fin-supports and fin-rays in the milkfish _Chanos chanos_. _Japanese Journal of Ichthyology_, _32_, 413–420.

Yamanoue, Y., Setiamarga, D. H. E., & Matsuura, K. (2010). Pelvic fins in teleosts: Structure, function and evolution. _Journal of Fish Biology_, _77_, 1173–1208.

Zhu, M., & Yu, X. (2009). Stem sarcopterygians have primitive polybasal fin articulation. _Biology Letters_, _5_, 372–375.

Ziermann, J. M., Freitas, R., & Diogo, R. (2017). Muscle development in the shark _Scyliorhinus canicula_: Implications for the evolution of the gnathostome head and paired appendage musculature. _Frontiers in Zoology_, _14_, 1–17.